Guided Wave Detection and Monitoring of Progressive Corrosion using Continuous Waves in Steel Pipelines with Macro Fiber Composite Transducers

Md Hasibur Rahman Kazi, Mohd Fairuz Bin Shamsudin*, and Fahad Bin Zahid

Abstract— **In the field of Structural Health Monitoring (SHM), corrosion is one of the main reasons for pipeline damage, which emphasizes the need for monitoring techniques capable of detecting wall thickness loss over long distances. This study examines the use of Macro Fiber Composite (MFC) transducers in generating and receiving Ultrasonic Guided Waves (UGW) in a pitch-catch orientation for corrosion monitoring. Unlike conventional tone-burst methods that rely on time-of-flight analysis, this study employs Continuous Wave (CW) steady-state excitation to exploit phase detuning and scattering sensitivity as corrosion damage indicators. The experiment was conducted on a 2.7m carbon steel pipe, with 2 axially bonded MFCs separated by 2.2m. Real accelerated and incremental corrosion was induced on the pipe using a 3wt.% NaCl solution with a constant current of 0.25 A which caused a total wall thinning of 2.118 mm. Continuous single-frequency sine waves at 20 kHz and 70 kHz at 1V peak to peak (1Vpp) were used to create a steady state guided wave field. Results show a consistent decrease in steady-state amplitude and signal integrity with respect to increasing corrosion. Analysis of cross-correlation metrics revealed that the 20 kHz signal decay is driven by phase detuning, whereas the 70 kHz signal degradation is driven by progressive scattering-related distortion and attenuation. These findings support that MFCs using continuous guided waves can detect corrosion-induced incremental thickness loss based on distinct, frequency-dependent guided wave phenomena.**

Keywords—Macro Fiber Composites (MFC), Structural Health Monitoring (SHM), Ultrasonic Guided Waves (UGW), Pipelines.

I. INTRODUCTION

Steel pipelines are a fundamental constituent for global energy and water distribution systems, yet they are highly prone to corrosion and degradation throughout their operational life. Corrosion is a leading cause of structural decline and failure, resulting in significant maintenance costs and safety risks worldwide [1]. Regular nondestructive techniques (NDTs) such as ultrasonic testing, magnetic flux leakage, and radiography provide accurate localized inspection, but require direct access to the pipe wall and point by point inspection, which makes them unsuitable for continuous, long-range structural health monitoring (SHM) [2].

Ultrasonic guided waves (UGWs) offer a suitable long-range option because they can cover long distances (tens of meters) while still being sensitive to wall thickness loss and corrosion-related defects. Their application in pipeline inspection is supported by extensive studies demonstrating sensitivity to material loss and geometric irregularities [3], [4], [5]. Despite this progress, many commercial systems rely on rigid and bulky piezoelectric collars or Electromagnetic Acoustic Transducer (EMATs), which can be difficult to use for permanent monitoring, especially in pipelines [6].

In terms of SHM in pipelines, Macro Fiber Composite (MFC) transducers can provide a suitable alternative. MFCs can bend and conform to curved surfaces due to their thin and flexible structure, and they can generate and sense guided waves precisely and efficiently due to their interdigitated electrode pattern within their structure [7]. Previous studies have shown the feasibility of using MFCs in pipelines [8]. However, most of the existing research is focused on artificial defects (e.g., machined slots) or qualitative observations rather than quantitative tracking of real and progressive corrosion [9]. Furthermore, prior MFC-based guided wave studies have mainly relied on tone-burst pulse excitation, leaving the steady-state continuous wave response largely unexplored as a monitoring option [8], [9]. Recent reviews emphasize the necessity for studies involving realistic corrosion to validate SHM durability and sensitivity [10].

To address these existing gaps in the literature, this study experimentally investigates the ability of MFC transducers to detect and monitor multi-stage progressive corrosion in a 2.7 m steel pipe. To achieve this, wall thinning across three severity stages was induced by localized electrochemically accelerated corrosion. Guided waves at 20 kHz and 70 kHz were chosen as the signals, and unlike pulse-echo methods that rely on time of flight [8], this study utilizes Continuous Wave (CW) excitations to examine the steady-state structural response. This approach enables the study to utilize the sensitivity of the steady-state guided-wave field which is sensitive to phase shifts and impedance mismatches, as well as the attenuation due to energy loss caused by localized thinning [11]. To systematically characterize signal deterioration, a Signal Similarity index is introduced which captures the combined effects of amplitude loss and phase detuning. In addition to that, a normalized Signal Distortion metric is also added which isolates pure waveform shape degradation independent of amplitude change.

The objective of this study is to demonstrate that surface-bonded MFC transducers, arranged in a pitch-catch configuration, can reliably detect and track corrosion progression over practical distances using CW steady-state excitation. The results provide new insights into the frequency dependent behavior of steady state guided waves in the presence of real corrosion, supporting the efficacy of MFC-based systems for pipeline SHM.

II. TECHNICAL BACKGROUND

UGWs in cylindrical structures propagate as a group of dispersive modes whose characteristics depend on geometry, material properties, and the excitation frequency. For pipeline inspection, the axisymmetric longitudinal modes L(0,1) and L(0,2) are widely used because they can cover long distances while remaining sensitive to cross-sectional changes and corrosion-related material loss [4]. Their sensitivity to thinning and geometric irregularities has been widely documented through analytical studies and controlled experiments [3]. Foundational work by Rose established the dispersion behavior, defect interaction mechanisms, and wavelength based scattering characteristics that drive guided wave responses in pipes [4], [12],[13].

When guided waves travel through corrosion-induced thickness loss, several methods of interaction contribute to measurable signal changes. These include energy loss due to scattering, mode conversion, and phase delay due to local velocity changes [14],[15]. Under CW excitation, the phase-related effects additionally appear as detuning of the steady-state guided-wave field which is a mechanism that is absent in conventional tone-burst approaches and represents a distinct sensitivity pathway exploited in this study. Here, detuning refers to a corrosion-induced phase shifting of the guided-wave interference field. As the wall thins, the local impedance change shifts the signal pattern relative to the fixed receiver, resulting in a measurable drop in the steady-state amplitude (Vp-p) that correlates with defect severity [10],[16]. At lower frequencies (e.g., 20 kHz) detuning/impedance changes usually dominate, whereas at higher frequencies (e.g., 70 kHz) scattering-related attenuation becomes much more significant [3],[4],[5].

Raghavan and Cesnik further emphasized that damage induced effects to guided-wave signals manifest both as amplitude changes and as subtle waveform distortions, supporting the use of correlation based analyses in SHM [17]. These principles justify examining both amplitude and waveform centric indicators in corrosion monitoring.

Because the MFCs are bonded to one side of the pipe, the excitation produces a multimodal guided-wave field containing longitudinal and flexural components, consistent with the behavior described by Giurgiutiu for surface-bonded piezoelectric actuators [18]. The received steady-state waveform therefore represents a combined modal response that remains sensitive to structural changes caused by corrosion.

MFCs are well suited for guided-wave generation in pipelines due to their interdigitated electrode structure, high in-plane actuation efficiency, and flexibility for bonding to curved surfaces. Their capability has been demonstrated in pipeline and plate studies showing effective excitation in the low and mid-frequency signals [8],[9],[10]. Notably, Thien et al. demonstrated the use of MFCs near 70 kHz for pipeline inspection, where short wavelengths produced strong interaction with localized defects [8]. Lower-frequency operation around 20 kHz is widely used for long-range screening because the dominant guided modes exhibit lower dispersion and often lower modal attenuation than higher-frequency modes [3],[4],[5].

Frequency selection plays an important role in determining which interaction mechanisms dominate the guided-wave response, and therefore evaluating which indicators are most effective at detecting and characterizing damage [19]. As guided waves in pipes are dispersive, the effective wavelength depends on both frequency and geometry. At 20 kHz, the effective guided-wave wavelength in steel pipes of similar geometry is approximately 250–270 mm, as reported by published disperse software-based dispersion analyses [20]. This wavelength is much larger than the 55 mm axial length of the corrosion patch, placing the interaction in a long wavelength and limited diffraction range where the initial thickness loss strongly affects the response, but sensitivity to further incremental corrosion gradually saturates. At 70 kHz, the effective wavelength is reduced to approximately 75–90 mm for the dominant longitudinal mode response [20], which is much closer to the defect dimensions and leads to an interaction driven by scattering and energy loss resulting in increased amplitude reduction and waveform distortion. These wavelength to defect relationships provide the physical basis for comparing corrosion sensitivity at 20 kHz and 70 kHz in this study.

III. Methodology

The experiment was conducted on a straight carbon steel pipeline instrumented with Macro-Fiber Composite (MFC) transducers. The methodology was designed to evaluate signal sensitivity low and mid-range frequencies during real electrochemical corrosion, measuring the degradation of the steady-state guided wave field as corrosion damage progressed.

A. *Experimental Configuration*

A 2.7 m long ASTM A106 Grade B steel pipe with an outer diameter of 114.3 mm and a thickness of 6.02 mm served as the test specimen. Two M2814-P2 MFC transducers were bonded axially to the external surface of the pipe with a separation distance of 2.2 m, forming a pitch-catch configuration (one MFC actuates the signal, the other MFC receives it). A localized corrosion region was created at the midpoint between the two MFCs.

As the MFCs were surface-bonded to only one side of the pipe, the excitation produced a multimodal guided-wave field consisting of longitudinal and flexural components. The MFCs were axially coincident which ensured that the propagating waves interacted with the central corrosion region before reaching the receiver. The overall schematic of the test section is illustrated in Fig. 1.

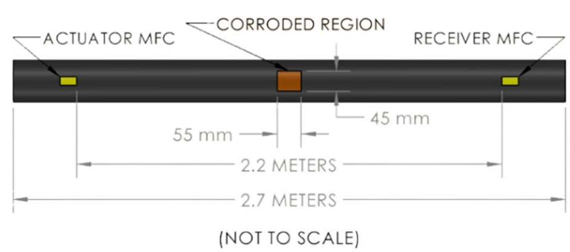

Fig. 1: Schematic overview of the pipe section

Prior to installation, bonding surfaces were polished, cleaned with acetone, and bonded using high-strength epoxy. Each MFC was electrically validated by capacitance measurement (approximately 43 nF) to confirm bond integrity.

B. *Accelerated Corrosion Process*

Realistic corrosion was induced electrochemically at the midpoint between the two MFCs. A localized external region (55 mm x 45 mm), amounting to an active area of approximately 25 cm², was enclosed within a sealed 3D printed cell made of Polylactic Acid (PLA), and filled with a 3 wt.% NaCl solution as the electrolyte. Silicone was used as the sealant to ensure zero leakage.

The pipe wall served as the anode and a graphite rod as the cathode, with a constant DC current of 0.25 A applied as shown in Fig. 2. Three sequential 72-hour corrosion cycles were conducted, each defining a corrosion stage (Stage 1–3), with Stage 0 as the undamaged baseline. After each cycle, deposits were removed and thickness loss was recorded using a precision micrometer at three circumferential locations, yielding average losses of 0.728 mm, 1.551 mm, and 2.118 mm at Stages 1, 2, and 3 respectively.

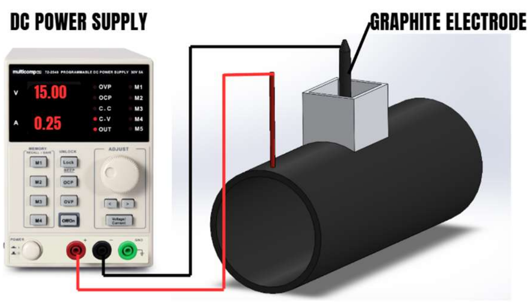

Fig.2: Corrosion Setup

C. Signal Generation and Acquisition

The complete experimental setup, from generation to acquisition, is shown in Fig. 3. The guided-wave signal was generated using a Tektronix AFG3021B arbitrary function generator. This low voltage signal was amplified by a PiezoDrive PX200 voltage amplifier and applied to the actuator MFC. The actuated signal then passed through the pipe and the corroded region and was received by the receiver MFC. The receiver MFC signal was then re-amplified and finally captured using a Rigol DHO914 digital oscilloscope at a sampling rate of 1.25 GSa/s. During signal acquisition, the room temperature was kept at a steady 25 °C for all stages.

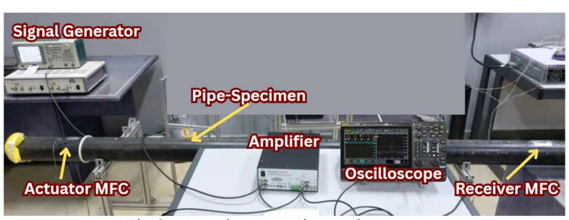

Fig.3: Complete experimental setup

Continuous single frequency excitation was selected to interrogate the steady-state structural response. Unlike transient tone-burst methods that isolate individual wave packets, this approach establishes a steady state sinusoidal wave field across the pipe length. This method was chosen to maximize the signal-to-noise ratio (SNR) and to utilize the high sensitivity of the steady-state sinusoidal wave pattern to phase shifts caused by localized impedance changes. Frequencies of 20 kHz and 70 kHz (1 Vpp) were selected to represent contrasting regimes: 20 kHz provides low-dispersion screening, while 70 kHz offers enhanced scattering sensitivity. For SNR computation, the noise floor voltage (Vpp_{noise}) was determined by recording the receiver MFC output with the excitation signal disabled, under otherwise identical acquisition conditions.

Both pipe ends were closed using foams of 25 mm thickness. This was done to reduce broadband reverberation, in the CW system, it stabilizes the boundary conditions to ensure a consistent steady-state field for comparative analysis.

D. Signal Processing

Signal processing was performed in Octave software. For each received signal, a time window was applied to isolate a suitable number of cycles of the steady-state sinusoidal region, ensuring the analysis focused on the CW field rather than transient wave packets. The peak-to-peak amplitude was computed to quantify attenuation. The SNR (signal to noise ratio) was also computed using the peak-peak voltage using the formula shown below to verify the quality of the signal.

$$SNR_{dB} = 20log_{10}\left(\frac{Vpp_{signal}}{Vpp_{noise}}\right) \quad (1)$$

To systematically evaluate signal degradation, two distinct correlation-based metrics were calculated relative to the Stage 0 baseline. First, a Signal Similarity (SS) index was defined to capture the combined effects of amplitude attenuation and phase shifting:

$$SS_i = \frac{max_\tau \langle x_0, x_i^\tau \rangle}{\|x_0\|^2} \quad (2)$$

Here, x_0 denotes the baseline signal and x_i^τ the signal at corrosion stage i shifted by a time lag τ. The numerator represents the maximum inner product between the baseline signal and the time-shifted response at stage i, while the denominator corresponds to the energy of the baseline signal. As this metric is normalized only by the baseline energy, it remains sensitive to the significant voltage drops fundamental to the detuning phenomenon.

Secondly, to isolate waveform shape distortion independent of amplitude loss, a percentage Signal Distortion (SD) was computed based on the standard Normalized Cross-Correlation (NCC):

$$NCC_{0i}(\tau) = \frac{\langle x_0, x_i^\tau \rangle}{\|x_0\|\|x_i\|} \quad (3)$$

$$\%SD_i = [1 - max_\tau\{NCC_{0i}(\tau)\}] \times 100\% \quad (4)$$

Here, $NCC_{0i}(\tau)$ denotes the normalized cross-correlation between the baseline signal and the time-shifted response at stage i. A % SD value of zero indicates a perfect waveform shape match, while increasing SD values quantify the loss of similarity due to scattering or other waveform distortions. Correlation-based metrics are widely used in guided-wave SHM because they are sensitive to phase shifts and subtle waveform deviation caused by structural damage. Waveform overlays were also examined to qualitatively visualize signal changes across corrosion stages. To ensure repeatability, each measurement was performed three times and the averaged values were used in the analysis.

IV. Results

The performance of the MFC-based guided-wave system was evaluated across three stages of progressive corrosion relative to the baseline condition. The results are presented in terms of measured thickness loss, steady-state signal amplitude (Vp-p), cross-correlation (CC), and waveform morphology. Collectively, these metrics demonstrate the capability of the experimental pitch-catch configuration to track structural degradation and impedance changes over a 2.2 m travel path on a 2.7 m pipe.

A. Quantification of Corrosion Severity

The accelerated corrosion process produced consistent and measurable wall thinning. As shown in Fig. 4, the first 72-hour cycle resulted in an average thickness loss of 0.728 mm. Following cycles increased the total loss to 1.551 mm (Stage 2) and 2.118 mm (Stage 3). These values represent early to moderate wall thinning and provide a consistent progression for evaluating sensor sensitivity.

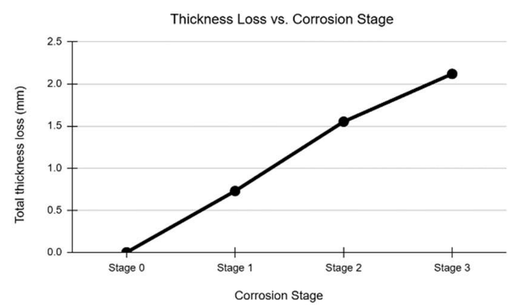

Fig.4: Thickness loss due to corrosion

B. Amplitude Response (Vp-p)

Guided-wave signals at both frequencies displayed significant amplitude reductions, though the trends differed due to wavelength dependent interaction mechanisms.

1) Low-Frequency Response (20 kHz):

For the 20 kHz excitation, the SNR was calculated to be 22.17 dB. The average baseline peak-to-peak amplitude was 1593 mV. Following Stage 1, the amplitude decreased sharply to 893 mV which is a 44% reduction. However, between Stage 1 and Stage 2, the amplitude plateaued, showing negligible change, before dropping to 675 mV at Stage 3. This is shown in Fig. 5.

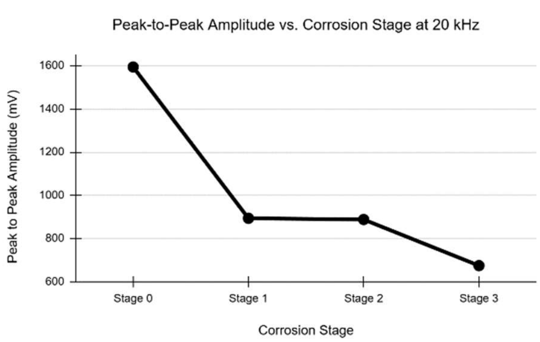

Fig.5: Amplitude vs Corrosion 20 kHz

This saturation behavior is characteristic of long-wavelength interactions in a steady-state field. The initial stage of corrosion significantly impacted the global impedance, shifting the guided wave pattern and reducing the amplitude at the receiver. However, because the 55 mm defect size is small relative to the estimated wavelength of 260 mm, further thinning produced diminishing changes in the wave field which led to the observed plateau. This suggests that at 20 kHz, detuning and impedance related effects dominate the amplitude trend, while attenuation contributes only weakly. Across all stages, the three repeated measurements showed standard deviations below 35 mV, confirming the stability and repeatability of the observed trends.

2) Mid-Frequency Response (70 kHz):

The SNR for the 70 kHz signal was calculated to be 26.64 dB. Amplitude measurements at 70 kHz ($\lambda \approx 75$ mm) showed substantially higher sensitivity to incremental thinning. The baseline amplitude of 2302 mV dropped to 1729 mV at Stage 1, then decreased sharply to 1230 mV at Stage 2 and 894 mV at Stage 3. This can be observed below in Fig. 6.

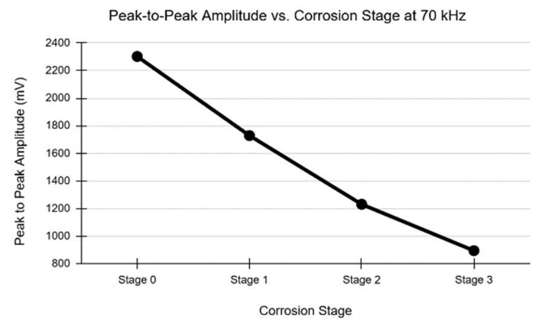

Fig.6: Amplitude vs Corrosion 70 kHz

At this frequency, the wavelength is comparable to the defect dimensions. This places the interaction in a system heavily influenced by scattering . Every millimeter of additional depth increased the local scattering, mode conversion and energy loss, resulting in a progressive amplitude reduction. This indicates that, in addition to impedance-related phase shifts, scattering-related attenuation plays a major role at 70 kHz. Repeated measurements yielded standard deviations below 50 mV across all stages, supporting the reliability of the observed progressive amplitude decline.

C. Signal Similarity and Waveform Distortion Analysis

While amplitude metrics quantify signal magnitude, two complementary cross-correlation indicators were evaluated to separate phase/impedance effects from waveform deterioration: the Signal Similarity index (SS), capturing combined attenuation and phase shift, and the percentage Signal Distortion (SD), isolating pure waveform shape distortion.

1) Signal Similarity (SS) Trends: As shown in Fig. 7, the SS index degraded significantly for both frequencies, mirroring the amplitude response.

- At 20 kHz: The index decreased from 1.000 to 0.585 at Stage 1, 0.529 at Stage 2, and 0.413 at Stage 3. Crucially, the SS metric continued to decrease between Stages 1 and 2 even when the amplitude plateaued. This indicates that while the signal magnitude stalled, the phase continued to shift due to the changing wall thickness..
- At 70 kHz: The SS index exhibited more consistent decline, dropping from 1.000 to 0.712 at Stage 1, then 0.480 at Stage 2, and finally 0.378 at Stage 3. This greater decline reflects the combined impact of attenuation and scattering at higher frequencies.

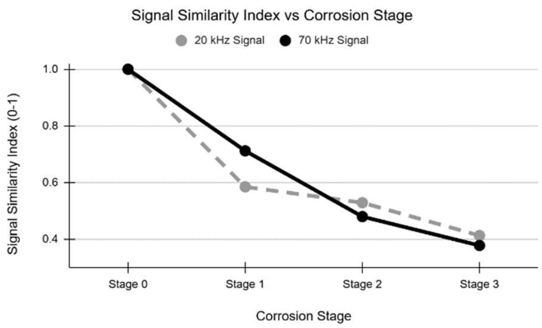

Fig.7: Signal Similarity Index vs Corrosion

2) Signal Distortion (SD): To identify the impacting damage mechanism, normalized cross-correlation based percentage SD was analyzed which is displayed in Fig. 8.

- At 20 kHz (Detuning): The % SD remained below 1% throughout all stages. Notably, the distortion actually decreased at Stage 3 to 0.43%, supporting that the wave retained its high sinusoidal correspondence with the baseline signal. This suggests that the massive drop in the SS metric is mostly driven by the spatial shifting caused by detuning of the steady state sinusoidal wave signals.
- At 70 kHz (Scattering): In contrast, the SD exhibited a consistent rise, increasing from near-zero to 1.59 % at Stage 3. This distinct upward trend confirms the onset of defect related scattering, where damage-induced mode conversion introduces noise that progressively distorts the waveform shape.

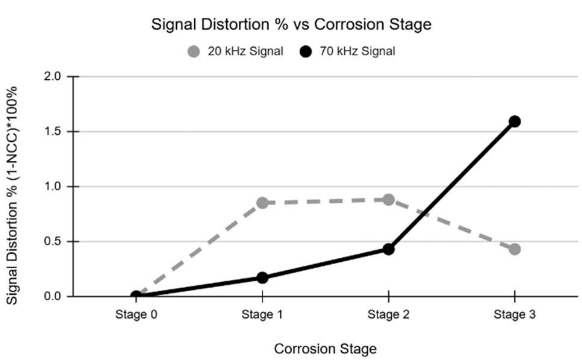

Fig.8: Signal Distortion vs Corrosion

3) Waveform Morphology: Waveform overlays further display the nature of these findings in a qualitative manner. The 70 kHz signal overlay throughout all the damage stages are displayed in Fig. 9. The Stage 0 waveform showed a clean sinusoidal shape with a high SNR, confirming the stability of the experimental setup. As corrosion progressed, the waveforms displayed clear amplitude reduction, slight phase offsets, and rounding of the peaks. Additionally, packets of high-frequency noise can also be observed in the signal. These distortions are consistent with the detuning and scattering phenomenon of a multimodal steady-state field caused by evolving boundary conditions at the corrosion site and the progressive thickness loss.

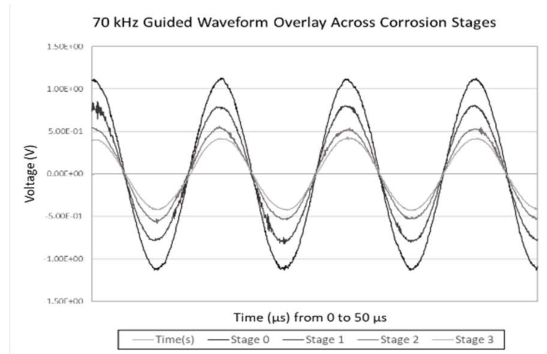

Fig.9: Waveform overlay 70 kHz

V. Discussion

The results support the conclusion that MFC transducers in a pitch-catch configuration can reliably detect progressive corrosion using CW steady-state signals. Signal reliability was verified by SNR values above 20 dB throughout all stages. At 70 kHz, amplitude dropped by over 60% across corrosion stages, demonstrating a strong correlation between wall-thickness loss and signal magnitude that validates the method's efficacy.

The characteristics of CW signals allow for the results observed in this study based on two co-existing phenomena. While the basics of guided-wave theory attribute amplitude reduction primarily to scattering and mode conversion at defect boundaries [3], using steady state signals introduces another sensitive mechanism. As the wall loses thickness, phase lag is induced by localized impedance changes, which spatially shifts the interference pattern relative to the fixed receiver location [18]. Thus, the measured amplitude loss is a combination of energy attenuation (scattering) and the spatial shifting of the wave field.

Actuation frequency was found to be the main factor determining which mechanism dominates, consistent with wavelength-defect interaction limits [4],[20]. At 20 kHz, the wavelength (~260 mm) greatly exceeds the 55 mm defect, causing the wave to skip through the corrosion patch once initial impedance contrast is established, producing the observed saturation plateau. At 70 kHz, the shorter wavelength (~75 mm) kept the interaction in the scattering regime, yielding a consistent progressive amplitude decline. This suggests lower frequencies are better suited for long-range screening, while 70 kHz is the more promising candidate for quantitative damage tracking in SHM.

Most importantly, the breakdown of the SS index and % SD helps clarify the distinction between these detection methods. At 20 kHz, the combination between the large drop in the SS index and the negligible rise in % SD indicates that the primary mechanism is detuning. On the other hand, at 70 kHz, the consistent rise in % SD is consistent with the strong effect of scattering. In this case, scattering is induced by the defects, introducing noise that progressively disturbs the waveform shape which was shown in Fig. 9. This multi-parameter analysis supports that combining amplitude with distortion metrics provides a reliable assessment of structural health, distinguishing between detuning and structural scattering.

Several limitations of this study should be acknowledged. The experiments were conducted in a controlled laboratory setting and on a single pipe specimen with a single corrosion location, which limits direct statistical generalization. While measurements were repeated three times at each stage to confirm repeatability, a broader multi-specimen validation would further strengthen confidence in the observed trends. The physical interpretation of detuning and scattering dominance, though consistent with established guided wave theory, was not supplemented by modal analysis or dispersion curve computation for the specific pipe geometry tested.

VI. Conclusion

The capability of MFC transducers to detect and monitor progressive and real corrosion in steel pipelines has been experimentally explored in this study. The system successfully tracked wall thickness loss from an early stage (0.7 mm) up until 2.1 mm by analyzing the steady-state structural response over a 2.2 m propagation distance.

The results support the conclusion that frequency selection is the main variable in assessing the monitoring performance, driven by two distinct physical mechanisms. A consistent and linear correlation was observed between the signal degradation and the corrosion depth for the 70 kHz signal. The % Signal Distortion (SD) strongly suggests that this response is driven by scattering, where mode conversions and energy loss progressively reduce waveform fidelity. This suggests 70 kHz as the most promising frequency for quantitative damage progression.

On the other hand, the 20 kHz mode displayed saturation effects consistent with diffraction limits. The analysis revealed that while amplitude dropped significantly, the waveform retained high sinusoidal fidelity and maintained a low % SD. This confirms that the low frequency response is mostly driven by the detuning of the steady-state signal rather than local scattering. Consequently, 20 kHz is best suited for qualitative long-range screening rather than damage quantification.

Future work will focus on validating this methodology with more frequencies, different waveforms and under complex operational conditions. Specifically, experiments will be conducted on pressurized pipes to evaluate how hoop stress affects the steady-state guided wave field and to simulate realistic in-service environments. Additionally, frequency-sweeping techniques will be explored to identify resonance shifts that could serve as supplementary damage indicators, further enhancing the robustness of the monitoring system.

Acknowledgment

This publication was also made possible by the support of Universiti Teknologi Malaysia under the research university grant UTMFR Q.J130000.3824.24H11.

References

[1] X. Chen and Y. Zhao, “Research on Corrosion Protection of Buried Steel Pipeline,” Engineering, vol. 9, no. 5, p. 504, Jan. 2017, doi: 10.4236/eng.2017.95030.

[2] R. K. Prodhan, M. M. Islam, and A. B. Fazle, “INTEGRATION OF ADVANCED NDT TECHNIQUES & IMPLEMENTING QA/QC PROGRAMS IN ENHANCING SAFETY AND INTEGRITY IN OIL & GAS OPERATIONS,” *American Journal of Interdisciplinary Studies*, vol. 3, no. 2, p. 1, Jun. 2022, doi: 10.63125/9pzxgq74.

[3] D. Alleyne and P. Cawley, “The interaction of Lamb waves with defects,” IEEE Transactions on Ultrasonics Ferroelectrics and Frequency Control, vol. 39, no. 3, p. 381, May 1992, doi: 10.1109/58.143172.

[4] J. L. Rose, Ultrasonic Guided Waves in Solid Media. Cambridge University Press, 2014. doi: 10.1017/cbo9781107273610.

[5] W. Luo, J. L. Rose, J. K. V. Velsor, M. J. Avioli, and J. Spanner, “Circumferential Guided Waves for Defect Detection in Coated Pipe,” AIP conference proceedings, vol. 820, p. 165, Jan. 2006, doi: 10.1063/1.2184525.

[6] A. M. Memon and L. M. Alhems, “EMAT Generated Guided Waves in Pipes,” e-Journal of Nondestructive Testing, vol. 28, no. 10, Oct. 2023, doi: 10.58286/28711.

[7] R. J. Williams, G. Park, D. J. Inman, and W. K. Wilkie, “An overview of composite actuators with piezoceramic fibers,” Nov. 2014, Accessed: Nov. 2025. [Online]. Available: http://citeseerx.ist.psu.edu/viewdoc/summary?doi=10.1.1.457.5202

[8] A. B. Thien, “Pipeline Structural Health Monitoring Using Macro-fiber Composite Active Sensors,” Jan. 2006, doi: 10.2172/883462.

[9] G. Ren and K.-Y. Jhang, “Application of Macrofiber Composite for Smart Transducer of Lamb Wave Inspection,” Advances in Materials Science and Engineering, vol. 2013, p. 1, Jan. 2013, doi: 10.1155/2013/281575.

[10] F. Lyu, X. Zhou, Z. Ding, X. Qiao, and D. Song, “Application Research of Ultrasonic-Guided Wave Technology in Pipeline Corrosion Defect Detection: A Review,” Coatings, vol. 14, no. 3, p. 358, Mar. 2024, doi: 10.3390/coatings14030358.

[11] S. Mariani and P. Cawley, “Change detection using the generalized likelihood ratio method to improve the sensitivity of guided wave structural health monitoring systems,” Structural Health Monitoring, vol. 20, no. 6, p. 3201, Dec. 2020, doi: 10.1177/1475921720981831.

[12] J. L. Rose, “A Baseline and Vision of Ultrasonic Guided Wave Inspection Potential,” Journal of Pressure Vessel Technology, vol. 124, no. 3, p. 273, Jul. 2002, doi: 10.1115/1.1491272.

[13] J. Mu, L. Zhang, J. L. Rose, and J. Spanner, “Long Range Ultrasonic Guided Wave Focusing in Pipe for Large Defect Circumferential Length Analysis,” AIP conference proceedings, vol. 894, p. 131, Jan. 2007, doi: 10.1063/1.2717964.

[14] P. Fromme, “Corrosion monitoring using high-frequency guided waves,” Proceedings of SPIE, the International Society for Optical Engineering/Proceedings of SPIE, vol. 9803, p. 980330, Apr. 2016, doi: 10.1117/12.2221893.

[15] A. C. Kubrusly, M. Freitas, J. P. von der Weid, and S. Dixon, “Interaction of SH guided waves with wall thinning,” NDT & E International, vol. 101, p. 94, Oct. 2018, doi: 10.1016/j.ndteint.2018.10.007.

[16] S. C. Olisa, M. Khan, and A. Starr, “Review of Current Guided Wave Ultrasonic Testing (GWUT) Limitations and Future Directions,” Sensors, vol. 21, no. 3. Multidisciplinary Digital Publishing Institute, p. 811, Jan. 26, 2021. doi: 10.3390/s21030811.

[17] A. Raghavan and C. E. S. Cesnik, “Review of Guided-wave Structural Health Monitoring,” The Shock and Vibration Digest, vol. 39, no. 2, p. 91, Feb. 2007, doi: 10.1177/0583102406075428.

[18] V. Giurgiutiu, “Tuned Lamb Wave Excitation and Detection with Piezoelectric Wafer Active Sensors for Structural Health Monitoring,” Journal of Intelligent Material Systems and Structures, vol. 16, no. 4, p. 291, Mar. 2005, doi: 10.1177/1045389x05050106.

[19] P. D. Wilcox, G. Konstantinidis, A. J. Croxford, and B. W. Drinkwater, “Strategies for Guided Wave Structural Health Monitoring,” AIP conference proceedings, vol. 894, p. 1469, Jan. 2007, doi: 10.1063/1.2718139.

[20] A. Demma, P. Cawley, M. J. S. Lowe, A. G. Roosenbrand, and B. Pavlakovic, “The reflection of guided waves from notches in pipes: a guide for interpreting corrosion measurements,” NDT & E International, vol. 37, no. 3, p. 167, Nov. 2003, doi: 10.1016/j.ndteint.2003.09.004.